Enviado para publicar por Elsevier: Fuel 86 (2007) 1036–1045

Operation of a 10 kW_{th} Chemical-Looping Combustor during 200 h with a CuO-Al_2O_3 Oxygen Carrier

Luis F. de Diego [a,*], Francisco García-Labiano[a], Pilar Gayán[a], Javier Celaya[a], José M. Palacios[b], Juan Adánez[a]

[a] *Instituto de Carboquímica (C.S.I.C.), Miguel Luesma Castán 4, 50018 Zaragoza, Spain.*

[b] *Instituto de Catálisis y Petroleoquímica, Campus UAM-Cantoblanco, 28049 Madrid, Spain*

RECEIVED DATE:

Corresponding_Author. Tel.: +34-976-733977; fax: +34-976-733318; *E-mail address*: ldediego@icbc.csic.es (L. F. de Diego)

Abstract

Chemical Looping Combustion (CLC) is an attractive technology to decrease greenhouse gas emissions affecting global warming, because it is a combustion process with inherent CO_2 separation and therefore without needing extra equipment for CO_2 separation and low penalty in energy demand. The CLC concept is based on the split of a conventional combustion of gas fuel into separate reduction and oxidation reactions. The oxygen transfer from air to fuel is accomplished by means of an oxygen carrier in the form of a metal oxide circulating between two interconnected reactors. A Cu-based material (Cu14Al) prepared by impregnation of γ-Al_2O_3 as support with two different particle sizes (0.1-0.3 mm, 0.2-0.5 mm) was used as an oxygen carrier for a chemical looping combustion of methane. A 10 kWth CLC prototype composed of two interconnected bubbling fluidized bed reactors has been designed, built in and operated at 800 ^oC during 100 h for each particle size. In the reduction stage full conversion of CH_4 to CO_2 and H_2O was achieved using oxygen carrier-to-fuel ratios above 1.5. Some CuO losses as the active phase of the CLC process were detected during the first 50 h of operation, mainly due to the erosion of the CuO present in external surface of the alumina particles. The high reactivity of the oxygen carrier maintained during the whole test, the low attrition rate detected after 100 hours of operation, and the absence of any agglomeration problem revealed a good performance of these CuO-based materials as oxygen carriers in a chemical-looping combustion process.

Keywords: Chemical-Looping Combustion; Oxygen carriers; Methane; Copper; CO_2 Capture

1. Introduction

According to the Intergovernmental Panel on Climate Change (IPCC), there is new and strong evidence that most of the global warming effect observed over the past 50 years is attributable to human activities. Moreover, CO_2 emissions mostly due to fossil fuel combustion, are determining on the observed increase of the atmospheric CO_2 concentration during the 21st century [1]. One of the options for reducing net CO_2 emissions to the atmosphere includes the capture and storage of this gas. Among the different technologies under development, Chemical-Looping Combustion (CLC) has been suggested as one of the most promising technologies for reducing the cost of CO_2 capture using fuel gas [1-2]. This combustion process, initially proposed by Ritcher and Knoche [3], allows beneficial exergy efficiencies of the system if CO_2 capture is considered [4]. Wolf et al. [5] reported a thermal efficiency as high as 52-53% achievable in a combined cycle CLC plant operating at 1200 ºC at 1.3 MPa in the air reactor, which represents a 5 percent more efficient process than a natural gas with combined cycle system using state-of-the-art technology for CO_2 capture. The efficiency would be something lower if an atmospheric CLC operating in a steam cycle is used.

CLC is a two-step gas combustion process that in the reduction stage produces a pure CO_2 stream, ready for further compression and sequestration. A solid oxygen carrier is circulated along two reactors, designated as air and fuel reactors, transporting oxygen available for combustion from air to fuel. In the fuel reactor (FR), the fuel gas reacts with a metal oxide (MeO) to give CO_2 and H_2O. As gas fuel can be used natural gas or synthesis gas from coal gasification. Since the fuel gas is not mixed with air subsequent CO_2 separation is, in fact, not necessary. The metal or reduced metal oxide is further transferred into the air reactor (AR) where it is oxidised with pure air, and the regenerated material is ready to start a new cycle. The outlet gas from the AR is made of N_2 and unreacted O_2. The outlet gas from the fuel reactor contains mainly CO_2 and H_2O. After water condensation, almost pure CO_2 can be obtained with little energy penalty from component separation. The net chemical reaction, and so the evolving heat, in a CLC process over the two

reactors is the identical to that occurring in a conventional combustion process, although the heat distribution between the FR and AR depends both on the fuel gas and the oxygen carrier.

Although several metal oxides (NiO, CuO, Fe_2O_3, etc.) can be used as oxygen carriers in a CLC process using CH_4 as fuel gas [6-7], the study in this work is focused in the use of copper based carriers. The main reactions taking place in the respective two reactors are the following:

FR	$4\ CuO + CH_4 \rightarrow 4\ Cu + CO_2 + 2\ H_2O$	$\Delta H_r^0 = -178$ kJ/mol	(1)
AR	$4\ Cu + 2\ O_2 \rightarrow 4\ CuO$	$\Delta H_r^0 = -624$ kJ/mol	(2)
Net	$CH_4 + 2\ O_2 \rightarrow CO_2 + 2\ H_2O$	$\Delta H_r^0 = -802$ kJ/mol	(3)

Cu-based oxygen carriers have several advantages: (1) CuO has a high oxygen transport capacity, allowing system operating with lower solid flow rates circulating between the FR and AR [8]. (2) Both the reduction and the oxidation reactions are exothermic (see above). Consequently, the involved solid flow rates necessary to fulfill heat balance is not as high as in other systems, as for example using NiO. (3) CuO reduction with methane is favored thermodynamically and the complete conversion of CH_4 into CO_2 and H_2O is possible; (4) CuO is one of the cheapest materials that can be used for CLC. (5) Cu-based materials are highly reactive, which reduce the solids inventory in the system [9], exhibiting additionally a good chemical stability.

The drawbacks reported in the literature for the use of these copper based oxygen carriers are: (1) The involved chemical species in the two stages of a CLC of methane are prone to exhibit thermal sintering since their melting points are close to the operating temperature used. This imposes limits to the maximum operation temperature used, 850 ºC, that reduces the efficiency of the CLC process. (2) This feature is also evidenced through the observed copper redistribution in multicycle tests in a fixed-bed reactor [10] and agglomeration problems found in fluidized bed reactors tests [11-12].

Although the advance of the CLC technology involved works carried out at different research levels, continuous operation in a CLC prototype is necessary to demonstrate the validity of this technology and to verify the usefulness of the particles developed. The CLC process was first successfully demonstrated by Lyngfelt et al. [13], and Lyngfelt and Thunman [14], in a 10 kW prototype during 100 h of continuous operation burning natural gas and using nickel-based oxygen carrier particles. Using NiO/bentonite carrier and CH_4 as fuel gas, Ryu et al. [15] demonstrated the inherent CO_2 separation, high CO_2 selectivity, high CH_4 conversion and no side reactions (carbon deposition and/or hydrogen generation) in a 50 kW chemical-looping combustor during a total operating time of more than 3.5 hours.

In this work, a 10 kW pilot plant composed of two interconnected bubbling fluidized bed reactors has been designed, built-in, and operated at 800 ^oC with a CuO/Al_2O_3 oxygen carrier during 200 h of continuous operation, 100 hours for each one of the two particle sizes tested. The paper has been focused especially on the analysis of the evolution of the oxygen carrier behaviour and structure during the operation test.

1.1. Previous work on copper based oxygen carriers

The key issue in the development of CLC technology is the oxygen carrier. Within the GRACE project, our research group developed a preliminary selection of oxygen carriers to be used in CLC. 240 samples composed up to 80 wt. % of Cu, Fe, Mn or Ni oxides on Al_2O_3, sepiolite, SiO_2, TiO_2 or ZrO_2, were prepared and tested [16]. On the basis of several properties including chemical reactivity, resistance to attrition, no agglomeration, etc., the most promising oxygen carriers based on nickel, iron, and copper were selected. Our research group, ICB-CSIC, continued the development of oxygen carriers based on copper because of the advantages above mentioned and ways to solve the operation problems found by other authors were found. The effects of the preparation method and carrier composition of Cu-based oxygen carriers were first analysed [17]. It was observed that to obtain high reactive oxygen carriers, maintaining the chemical and mechanical properties during a

high number of reduction/oxidation, the optimum preparation method for Cu-based oxygen carriers is the impregnation on a support. Later, the preparation conditions and oxygen carrier characteristics (including MeO content, calcination temperature, etc.) were optimised to avoid the agglomeration of the Cu-based materials during their operation in a fluidized bed [18], which was the main reason adduced in the literature to reject this kind of materials for their use in a CLC process. These materials were tested during multicycle tests in thermobalance and batch fluidised bed tests. Moreover, Cu-based oxygen carriers prepared by impregnation are very reactive, which leads to small solid inventories in the process [9]. An oxygen carrier was finally selected to test its behaviour at larger scale during continuous operation, which corresponds to the work herein presented.

2. Experimental Section

2.1 Oxygen carrier preparation.

Commercial γ-Alumina (Puralox NWa-155, Sasol Germany GmbH) particles of 0.1-0.3 and 0.2-0.5 mm was used as support in the preparation by incipient wet impregnation of 60 kg of a Cu-based oxygen carrier (Cu14Al) with a CuO content of 14 wt%, half for each one of the two particle sizes batches tested in the plant.

The oxygen carrier was prepared by adding a volume of an aqueous solution of copper nitrate 5 M necessary to fill up the total pore volume of the porous support (4.2×10^{-4} m^3/kg). The oxygen carrier was subsequently calcined for 30 min at 550 ºC in a muffle oven to decompose the copper nitrate into copper oxide. Afterwards, to get proper stability at the CLC operating conditions, the oxygen carrier was calcined at 850 ºC for 1 hour prior to test.

Table 1 shows the main properties of the fresh oxygen carrier, as well as the obtained after 100 h of continuous operation in pilot plant tests. The characteristics of the inert support were also included for comparison. This Table also includes an important characteristic of any oxygen carrier as it is the oxygen transport capacity, Ro, that is, the mass fraction of oxygen that can be used in the

oxygen transfer process. This property was defined as $R_o=(m_{ox}-m_{red})/m_{ox}$, where m_{ox} and m_{red} are the masses of the oxidised and reduced form of the metal oxide, respectively.

2.2 Oxygen carrier characterization

Samples of oxygen carrier taken from different locations in the plant and at different operation times were characterized by using several techniques. Reactivity tests were carried out by thermogravimetic analysis (TGA). Detailed information about the thermobalance (CI Electronics Ltd.) and operating procedure used can be found elsewhere [7]. Carrier porosity was measured by Hg intrusion in a Quantachrome PoreMaster 33, and the BET specific surface area was determined by N_2 physisorption in a Quantachrome Autosorb-1. The identification of crystalline chemical species was carried out by powder X-ray diffraction (XRD) patterns acquired in an X-ray diffractometer Bruker AXS D8ADVANCE using Ni-filtered Cu Kα radiation equipped with a graphite monochromator. The copper distribution in a cross section of a particle embedded in resin epoxy was determined in a scanning electron microscope (SEM) ISI DS-130 coupled to an ultra thin window PGT Prism detector for energy-dispersive X-ray (EDX) analysis.

2.3 Experimental CLC prototype

The schematic diagram of the 10 kWth Chemical-Looping Combustor used is shown in Figure 1. The plant was designed to facilitate the introduction of changes in the solid flow rates keeping the fuel-to-oxygen ratio constant. In this way, the study of the effect of this parameter on the combustion efficiency is straightforward. The FR (1) consisted in a bubbling fluidized bed (0.1 cm i.d.) with a bed height of 0.5 m and a freeboard of 1.5 m. In this reactor the methane reacts with the oxygen carrier to give CO_2 and H_2O (see Equation 1). The furnace surrounding the FR (10) was used for necessary heating during the start-up period and eventual counterbalancing of heat losses allowing accurate control of the operating temperature. The solids previously reduced in the FR were then transported to the AR (2) through a loop seal fluidized bed reactor (3a). The regeneration of the

oxygen carrier took place in the AR (see Equation 2) allowing residence times high enough for achieving the complete oxidation of the reduced carrier. It consisted of a bubbling fluidized bed (0.16 m i.d.) with a bed height of 0.5 m and a freeboard of 1 m.

The fully oxidized carrier was taken up by a pneumatic system (4), recovered by a high-efficiency cyclone (5), and sent to a solid reservoir (6) setting the solid ready to start a new cycle. The outlet gas from the AR, composed of N_2 and unreacted O_2, was sent to stack. The regenerated oxygen carrier returned to the FR by gravity from the solid reservoir (6) located above a solids valve (7) which controlled the flow rates of solid entering the FR. A diverting solids valve (8) located below the cyclone allowed the measurement of the solid flow rates at any time. The fines produced by fragmentation/attrition in the plant were recovered both in the cyclones and filters (9) located in the FR and riser lines.

There are two loop seals in the system to avoid solids back flow and gas mixing between reactors. A nitrogen-flowing loop seal (3a) prevented mixing of the fuel gas in FR and the oxygen in AR while solids were flowing through it.

The prototype was provided with several tools of measurement and system control. Thermocouples and pressure drop transducers located at different points of the plant showed the current operating conditions in the plant at any time. Accurate flow rates of feeding gases were obtained by means of specific mass flow controllers. The gas outlet streams of the FR and AR were drawn to respective on-line gas analysers to get continuous data of the gas composition. CH_4, CO, H_2, and CO_2 concentrations in the gas outlet stream from the FR were obtained after steam condensation. CO, CO_2, and CH_4 concentrations were measured using non-dispersive infrared (NDIR) analysers (Maihak S710 / UNOR), O_2 concentration was determined using a paramagnetic analyser (Maihak S710 / OXOR-P), and H_2 concentration by using a thermal conductivity detector (Maihak S710 / THERMOR). All data was collected by means of a data logger connected to a computer.

3. Results and Discussion

CLC tests using the Cu-based oxygen carrier and methane as fuel gas were carried out in the 10 kWth CLC prototype at different operating conditions. The solid inventory in the whole system was about 21 kg and the solid flow rates were varied between 60 and 250 kg/h. The usual operating temperature was 800 ºC and the linear gas velocities at the FR and AR inlets were 0.1 and 0.5 m/s, respectively. It is worth noting that the gas velocity in FR increases by a factor of 3 as a consequence of the stoichiometry of the reduction reaction with CH_4 (see Equation 1). Some additional tests were carried out to study the effect of the operating temperature in the range of 700 - 800 ºC and of the linear velocities in the range of 0.07 – 0.14 m/s. Temperatures in FR and AR were accurately kept constant during operation.

Prototype tests were conducted using two different particle sizes (0.2-0.5 mm, 0.1-0.3 mm) for 200 h including the start-up periods. Each particle size test was run for 100 h from which 60 h corresponded to the combustion period. Reactor tests showed that the most important parameter in CLC process was the oxygen carrier-to-fuel ratio used in FR. It must be kept in mind that, for Cu-based oxygen carriers, both the reduction with CH_4 and the oxidation are exothermic. Therefore, the solid flow rates in the system are mainly based on the oxygen necessary to achieve high CH_4 conversions and are not limited by the heat balance as happens with other Fe- and Ni-based oxygen carriers [8].

The effect of the oxygen carrier-to-fuel ratio on fuel conversion, for a constant air to fuel ratio (1.2), is shown in Figure 2. This parameter was defined by accounting for the stoichiometry of the reduction reaction (see Equation 1). A value of 1 corresponded to a flow rate of oxygen carrier providing the oxygen necessary to get complete CH_4 conversion. Low CH_4 conversions were obtained by using sub-stoichiometric ratios (<1) and, additionally, important CO and H_2 concentrations, besides unconverted CH_4, were also detected in the FR gas outlet stream. Moreover, the presence of small CO_2 concentrations detected in the outlet gas from the AR suggest the probable carbon formation in the prior reduction stage through CH_4 thermal decomposition. At oxygen carrier to fuel ratios lower than 1, the lack of enough available oxygen in the reduction stage

not only leads to small CH_4 conversions but enhances the occurrence of unwanted side reactions. The CH_4 conversion increased rapidly as this parameter rise and for ratios above 1.5 complete conversion of methane to CO_2 and H_2O was achieved. With respect to the solid, as the solids flow rate increases, the change in solid conversion decreases. As a consequence, the oxygen carrier has a higher capacity to convert methane to a higher extent in the fuel reactor. These results prove the validity of Cu-based materials as oxygen carriers for a CLC process in a pilot plant under continuous operation avoiding the use of additional stages for CO_2 purification before storage. Moreover, no CO and/or CO_2 were detected in the AR outlet stream indicating no leakage between reactors and no carbon deposition in the FR.

3.1 Mass balance

A mass balance of the oxygen carrier was carried out in the prototype over the whole period of experimentation. Since similar operation procedures and conclusions were obtained for the two particle sizes used, the results corresponding to the higher particle size distribution are showed in Table 2, as an example. The pilot plant was filled with 21 kg of oxygen carrier and the solid flow rates kept constant during 4 hours at 500 ºC to remove the solid fines produced during preparation. After this initial operation, the total solids inventory in the system was increased, especially to fill the solid reservoir located above the solids valve since it allowed a better control of the solids circulation flow and the gas leakage between reactors. The operation with this particle size was carried out during a period of 11 days. Samples of oxygen carrier were taken every day for analysis.

Mass balance of CuO was obtained from samples taken from the system at different times and the CuO concentration determined by TGA using H_2 as reducing gas. TGA analysis included samples extracted from the reactors bed as well as solids elutriated and recovered in cyclones and filters. Most of the material elutriated was recovered in the cyclone located after AR and the filter located downstream the riser. The mass elutriated from the FR was comparatively negligible. The total

amount of solids elutriated from the prototype after 100 hours of operation corresponded to carrier loss of ~7 %. The mass balance was fulfilled within a 5 % of standard deviation.

Additional and interesting information was gained from the mass balance of copper. It was observed that the elutriated fines were concentrated in CuO with respect to the existing levels found in the reactors. It means that the CuO content in the oxygen carrier of the reactors was progressively decreasing with time. After 50 h of operation, the CuO content in the carrier stabilized in values about 10 % and no significant decrease in CuO content was observed later. This CuO loss was also observed in the tests carried out with the particle size 0.1-0.3 mm. In this case, the CuO content was stabilized in values about 9.5 %.

3.2 Agglomeration

Cu-based oxygen carriers had been rejected in the past as potential candidates for CLC as a consequence of the particles agglomeration observed during operation in fluidized bed reactors [11-12]. However, the oxygen carrier tested in this CLC prototype was prepared according to the manufacture conditions proposed by de Diego et al. [18] to prevent the occurrence of agglomeration problems. This Cu-based material never presented agglomeration problems during operation at the CLC prototype in complete agreement with the results obtained previously by de Diego et al. [18] in a smaller scale reactor.

3.3 Attrition

The number of successive reduction-oxidation cycles withstood by an ideal oxygen carrier would be infinite. However, the oxygen carrier material must be renovated because of particle attrition/fragmentation during successive reduction-oxidation cycles and a new makeup flow of new material is necessary. In economical terms, the cost of this additional feeding is not significant to the

overall cost of the process [8], although the attrition rate of the material could affect to the solids filtration system of the CLC plant.

To determine these effects, the particle size distribution present at different locations of the prototype and at different times was first determined (see Table 3). The average particle size of the oxygen carrier in the FR bed decreases after 100 h of operation as a consequence of the attrition/fragmentation of large particles, and also to the possible shrinking of the particles by internal phase changes. Moreover, fine particles with size below 100 μm, not present in the fresh material, were elutriated from the reactors and collected in the respective cyclones and filters located downstream.

Figure 3 shows the evolution of the attrition rate of the carrier particles during the whole operation in the prototype. The values have been calculated assuming as attrition those particles recovered in cyclones and filters of size under 40 μm. The generation of fine particles was high at the beginning of the operation but, then, a sharp decrease was observed. After 50 hours of operation a low and constant value of the attrition rate was apparently reached (~0.04 wt% h^{-1}) for the two particle sizes used in the tests. Assuming that as a measure of the of the steady-state attrition, a particle lifetime of ~2400 hours was inferred; that is, the solids inventory in the CLC plant must be replaced ~3.4 times a year. These values should even be better in an industrial CLC plant where the solids recovered in the cyclones are returned to the system.

3.4 Reactivity

Since in every cycle of CLC the oxygen carrier undergoes important chemical and structural changes at high operating temperature, substantial changes in the reactivity with the number of cycles might be expected. The reactivity of the fresh oxygen carrier as well as the carrier existing in the prototype at different operation times was analyzed by TGA. A gas composed of 15 vol% CH_4 and 20 vol% H_2O for the reduction and pure air for the oxidation were used. Figure 4 shows the

evolution of the oxygen transport capacity of the carriers in reactivity tests carried out in thermobalance at 800 °C for the higher particle size tested (0.2-0.5 mm). This Cu-based oxygen carrier showed high reactivities both in reduction and oxidation stages with reaction times for complete conversion lower than 20 s. Moreover, the samples maintained these high reactivities along 100 h of operation in the prototype. This high reactivity was also maintained for the other particle size tested in the prototype, 0.1-0.3 mm. However, some loss in the oxygen transport capacity up to 50 hours of operation was evidenced because of the decrease on the CuO content of the carrier, as shown in Table 2. For the particle size of 0.2-0.5 mm, this property was stabilized in a value about 0.017 grams of oxygen per gram of material, which corresponds to a CuO content in the oxygen carrier of ~10 wt%. For the smaller particles used, 0.1-0.3 mm, the CuO content after 100 hours of operation was ~9.5 wt%.

3.5 Characterization study of the fresh and used oxygen carriers

The evolution of the textural and structural properties of the oxygen carriers were studied by Hg porosimetry, N_2 physisorption, XRD, and SEM-EDX in samples extracted from the prototype at different times. Table 1 shows the main properties of the oxygen carrier both fresh and after operation. The BET specific surface area decreased from ~80 m^2/g in the fresh carriers after calcination to ~33 m^2/g just after the first hours of reaction. The carrier porosity decreased from ~54 % to ~52.0 % after 100 h operation with the respective mean pore size shifting towards pores of higher size, as shown in Figure 5. These features suggest that some accumulative thermal sintering is occurring in the carriers along the prototype tests but, fortunately, they did not affect the carrier reactivity, as shown in Figure 4.

Powder XRD patterns of the fresh carrier, shown in Figure 6, revealed the presence of $CuAl_2O_4$, and γ-Al_2O_3 as major crystalline phases and minor amounts of CuO. The presence of this mixed oxide indicates that CuO interacted strongly with the support forming the spinel phase $CuAl_2O_4$ during calcinations by solid-state reaction. The appearance of broad reflections of the γ-Al_2O_3

indicates that it is microcrystalline with small domain sizes. On the contrary, the reflections of the spinel phase ($CuAl_2O_4$) are thin, which indicates that the crystalline domains are big (>0.1 μm). The powder XRD patterns of used carriers after different operation times revealed the presence of the same crystalline phases with two substantial differences to those found in the fresh oxygen carrier: a) γ-Al_2O_3 progressively evolved to α-Al_2O_3 as a most stable phase at high temperature. b) The CuO content was significantly higher than that found in the fresh carrier and did not change substantially with the operation time. The progressive transformation of γ-Al_2O_3 into α-Al_2O_3 can explain the observed evolution of the textural properties of used carriers. The strong interaction of CuO with alumina through the formation of $CuAl_2O_4$ and the simultaneous presence of CuO implies that both phases are active for reduction. TGA tests revealed that the reactivity of the CuO and the spinel phase was high at 800 ^oC (see Figure 4).

The oxygen carrier particles were also analysed by SEM-EDX. Figure 7 shows the images of the particles before and after operation. As shown in Figures 7a) and 7b), the oxygen carrier particles exhibited an irregular shape although the corners of the used particles were rounded by the attrition suffered during operation. Fresh oxygen carrier had the external surface covered by small grains of CuO (Figure 7c). Most of these grains were separated from the particles by attrition and elutriated during operation. Images corresponding to particles with 15 hours of operation time showed a decreasing content of these CuO grains in the surface, and almost disappeared after 35 hours of reaction. In the last case, the general appearance of the particles was similar to the obtained after the 100 hours test (see Figure 7d). This fact qualitatively agrees with the CuO loss observed in the particles during the first operation stages and the simultaneous CuO enrichment observed in the elutriated small particles recovered in cyclones and filters. As showed in Table 2, the CuO content of the particles decreased from 14 % in the fresh particles to about 11.5 wt% after 35 hours of reaction. However, it is difficult to know if the loss of the external CuO grains corresponds to the total CuO loss observed by the mass balance. It must be remembered that copper species, especially CuO in the regeneration stage of CLC process, tends to migrate to the external surface of the carrier particles

[10]. To analyse if this effect could affect to the copper distribution inside the particles, some particles were embedded in resin epoxy, cut, polished and analysed by EDX. Fresh particles clearly exhibited an outer shell of CuO (Figure 7e), which disappeared for the reacted particles (Figure 7f). This fact was also corroborated by the EDX analysis carried out to the particles. SEM-EDX line profiles revealed two high peaks of Cu corresponding to the external shells of the fresh particles (Figure 7g), which were not found in any case after 100 hours of reaction (Figure 7h). This analysis also showed that the Cu continued uniformly distributed inside the particle, as happened in the fresh particles. However, it was not possible to quantify the change in the internal Cu content during operation in the CLC prototype.

The analysis carried out to the particles demonstrates that Cu-based materials can be used as oxygen carriers in a CLC plant because they allow the full conversion of the fuel gas CH_4 into CO_2 and H_2O maintaining their properties after 100 h of continuous operation (high reactivity, no agglomeration, low attrition, etc.). The improvement of the preparation method to avoid the existence of CuO grains in the external surface of the particles will improve the characteristics of these Cu-based materials.

Conclusions

A 10 kWth Chemical-Looping Combustion prototype based on two interconnected fluidized beds has been designed, built and satisfactorily operated with CH_4 during 200 h at 800 ºC with a copper-based oxygen carrier prepared by impregnation.

The tests showed that the most important parameter in a CLC process was the oxygen carrier-to-fuel ratio used. In this sense, complete conversion of CH_4 into CO_2 and H_2O was obtained in the fuel reactor for ratios above 1.5. The absence of CO and CO_2 in the air reactor outlet stream demonstrated the good performance of the prototype since gas leakage between reactors and carbon deposition in FR were absolutely avoided.

The mass balance carried out during the tests revealed the loss of CuO in the oxygen carrier particles during operation at high temperature, especially during the first 50 hours. The analysis of the particles revealed that an important CuO loss fraction corresponded to the CuO grains present in the external surface of the fresh particles. However, the performance of the Cu-based oxygen carrier was excellent. The particles maintained a high reactivity, both during reduction and oxidation, after the 100 hours of continuous operation for each one of the particle size used. The attrition rate, although high initially, was stabilized in values rather low, and the material never presented agglomeration problems. Therefore, this work is the first demonstration of the good performance exhibited by any Cu-based material operating at high temperature in a continuous CLC process.

Acknowledgements

This research was carried out with financial support from the Spanish Ministry of Education and Science (Projects PPQ-2001-2111 and CTQ-2004-04034) and from the Diputación General de Aragón (Project PIP023/2005).

References

[1] IPCC special report on carbon dioxide capture and storage (2005). Available at http://www.ipcc.ch.

[2] Kerr HR. Capture and separation technologies gaps and priority research need. In Carbon Dioxide Capture for Storage in Deep Geologic Formations - Results from the CO_2 Capture Project; Thomas, D., Benson, S., Eds.; Elsevier Science: Oxford, 2005; Vol. 1, Chapter 38.

[1] Ritcher H, Knoche K. Reversibility of combustion process. ACS Symposium Series 1983; 235:71-85.

[4] Wolf J, Anheden M, Yan J. Comparison of nickel- and iron-based oxygen carriers in chemical looping combustion for CO_2 capture in power generation. Fuel 2005; 84:993-1006.

[5] Wolf J, Anheden M, Yan J. Performance analysis of combined cycles with chemical looping combustion for CO_2 capture. Proceedings of the 18th Annual International Pittsburg Coal Conference, NewCastle, New SouthWales, Australia; 2001; pp. 1122-1139.

[6] Ishida M, Zheng D, Akehata T. Evaluation of a chemical-looping combustion power-generation system by graphic exergy analysis. Energy 1987;12:147-154.

[7] Mattisson T, Lyngfelt A. Capture of CO_2 using chemical-looping combustion. Proceedings of the Scandinavian-Nordic Section of Combustion Institute, Göteborg, Sweden; 2001.

[8] Abad A, Adánez J, García-Labiano F, de Diego LF, Gayán P, Celaya J. Mapping of the range of operational conditions for Cu-, Fe-, and Ni-based oxygen carriers in chemical-looping combustion. Chem Eng Sci 2006; in press

[9] García-Labiano F, de Diego LF, Adánez J, Abad A, Gayán P. Reduction and oxidation kinetics of a copper-based oxygen carrier prepared by impregnation for chemical-looping combustion. Ind Eng Chem Res 2004;43:8168-8177.

[10] Corbella BM, de Diego LF, García-Labiano F, Adánez J, Palacios JM. Characterization and performance in a multicycle test in a fixed-bed reactor of silica-supported copper oxide as oxygen carrier for chemical-looping combustion of methane. Energy Fuels 2006;20:148-154.

[11] Copeland R, Alptekin G, Cesario M, Gershanovich Y. Sorbent energy transfer system (SETS) for CO_2 separation with high efficiency. Proceedings of the 27th Int. Tech. Conference on Coal Utilization & Fuel systems, Ed: CTA, Clearwater, Florida, USA, 2002; pp. 719-729.

[12] Cho P, Mattisson T, Lyngfelt A. Comparison of iron-, nickel-, copper and manganese-based oxygen carriers for chemical-looping combustion. Fuel 2004;83:1215-1225.

[13] Lyngfelt A, Kronberger B, Adánez J, Morin J.-X, Hurst P. The GRACE project. Development of oxygen carrier particles for chemical-looping combustion. Design and operation of a 10kW chemical-looping combustor. Proceedings of the 7th International Conference on Greenhouse Gas Control Technologies, Vancouver; 2004.

[14] Lyngfelt A, Thunman H. Construction and 100 h operational experience of a 10-kW chemical looping combustor. In Carbon Dioxide Capture for Storage in Deep Geologic Formations - Results from the CO_2 Capture Project; Thomas, D., Benson, S., Eds.; Elsevier Science: Oxford, 2005; Volume 1, Chapter 36.

[15] Ryu HJ, Jin GT, Yi CK. Demonstration of inherent CO_2 separation and no NO_x emission in a 50 kW chemical-looping combustor: Continuous reduction and oxidation experiment. Proceedings of the seventh international conference of greenhouse gas control technologies, Vancouver, Canada, September; 2004.

[16] Adánez J, García-Labiano F, de Diego LF, Gayán P, Abad A, Celaya J. Development of oxygen carriers for chemical-looping combustion. In Carbon Dioxide Capture for Storage in Deep Geologic Formations - Results from the CO2 Capture Project; Thomas, D., Benson, S., Eds.; Elsevier Science: Oxford, 2005; Volume 1, Chapter 34.

[17] de Diego LF, García-Labiano F, Adánez J, Gayán P, Abad A, Corbella BM, Palacios JM. Development of Cu-based oxygen carriers for chemical-looping combustion. Fuel 2004;83:1749-1757.

[18] de Diego LF, Gayán P, García-Labiano F, Celaya J, Abad A, Adánez J. Impregnated CuO/Al_2O_3 oxygen carriers for chemical-looping combustion: avoiding fluidized bed agglomeration. Energy Fuels 2005;19:1850-1856.

Table 1.Properties of the Cu-based oxygen carrier.

	γ-Al_2O_3	Cu14Al			
		dp = 0.1-0.3 mm		dp = 0.2-0.5 mm	
		Fresh	After 100 h	Fresh	After 100 h
Active material (%)		14	9.5	14	10
Ro (%)		2.7	1.7	2.7	1.8
Porosity	55.4	54.8	52.1	53.7	52.0
Apparent density (kg/m^3)	1300	1500	1620	1560	1650
BET specific surface area (m^2/g)	155	80.5	34.9	77.3	31.7

Table 2. Mass balance for the operation carried out with the Cu14Al oxygen carrier. dp = 0.2-0.5 mm.

Total time (h)	Time under combustion	Oxygen carrier mass balance (g OC)				CuO balance (g CuO)		
		In	Out			In	Out by sampling and losses	CuO (%) in system [b]
	h		sampling	loss FR	loss AR and riser [a]			
0	0	21000	0	0		2940		14
4	0		50	15	219		166	13.5
15	8	2000	50	20	466	280	321	12.5
24	13		50	10	310		189	11.5
34	21		50	9	226		109	11.3
41	25	1000	50	10	98	140	53	11.1
50	30	1000	50	6	78	140	36	10.5
60	37		50	9	94		45	10.5
70	44		50	8	75		35	10.5
79	51		50	6	89		29	10.0
88	57		50	12	105		23	10.0
100	65		50	9	115		23	10.0
TOTAL		**25000**	**550**	**114**	**1875**	**3500**	**1029**	

a. including solids from filters and AR cyclone.

b. determined by TGA analysis

Table 3. Particle size distribution of the particles present at different locations at times.

	dp=0.1-0.3 mm				dp=0.2-0.5 mm			
	Initial	After 100 h operation			Initial	After 100 h operation		
	Bed	Bed	AR Cyclone	Filter	Bed	Bed	AR Cyclone	Filter
400 - 500					12. 7	7.5		
300 - 400					71.3	56.0		
200 - 300	81.2	65.6			16.0	35.3		
100 - 200	18.8	32.9				1.2		
74 - 100		1.5	17.6				1.2	2.0
63 - 74			8.4	5.3			1.2	0.2
40 - 63			20.7	8.5			3.0	7.3
25 - 40			50.2	23.1			28.8	17.7
< 25			3.1	63.1			65.8	72.8

Captions of the Figures

Figure 1. Schematic diagram of the CLC prototype. (1) fuel reactor; (2) air reactor; (3) loop seals; (4) riser; (5) cyclone; (6) solid reservoir; (7) solids valve; (8) diverting solid valve; (9) filters; (10) oven; (11) air preheater; (12) water condenser.

Figure 2. Effect of the oxygen carrier-to-fuel ratio on the CH_4 conversion. T = 800 ºC, u = 0.1 m/s. dp=0.2-0.5 mm.

Figure 3. Evolution of the attrition rate of the Cu14Al oxygen carrier.

Figure 4. Evolution of the reduction and oxidation reactivities of the carrier Cu14Al-I along a 100 h prototype test. dp=0.2-0.5 mm.

Figure 5. Evolution of the pore size distribution of the oxygen carrier Cu14Al-I during CLC operation.

Figure 6. Powder XRD patterns of the oxygen carrier extracted at different operation times from the fluidized reactor bed.

Figure 7. SEM-EDX images of the oxygen carrier particles both fresh and after 100 h of operation. a) and b) SE (secondary electrons) image of the particles; c) and d), BSE (back-scattering electrons) photograph of a particle; e) and f), BSE image of a cross section of a particle; g) and h) EDX line profiles of Cu in a particle.

Figure 1

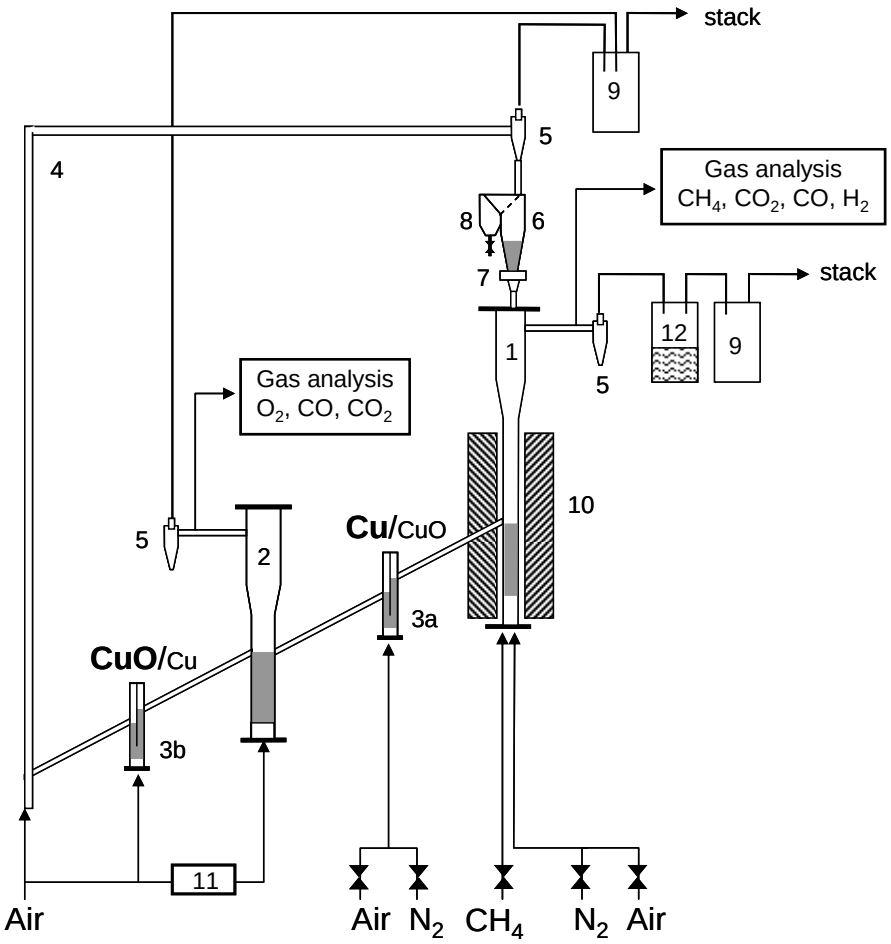
stack
9
5
4
Gas analysis
CH4, CO2, CO, H2
8
6
7
stack
12
9
1
5
Gas analysis
O2, CO, CO2
10
5
2
Cu/CuO
3a
CuO/Cu
3b
11
Air
Air
N2
CH4
N2
Air

Figure 2

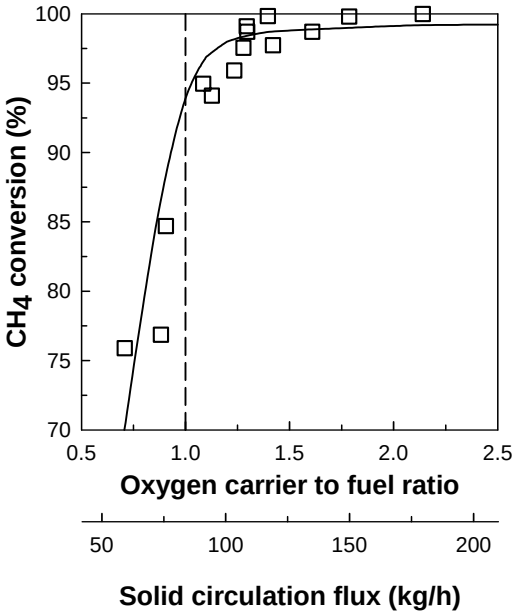
100
95
90
85
80
75
70
CH4 conversion (%)
0.5
1.0
1.5
2.0
2.5
Oxygen carrier to fuel ratio
50
100
150
200
Solid circulation flux (kg/h)

Figure 3

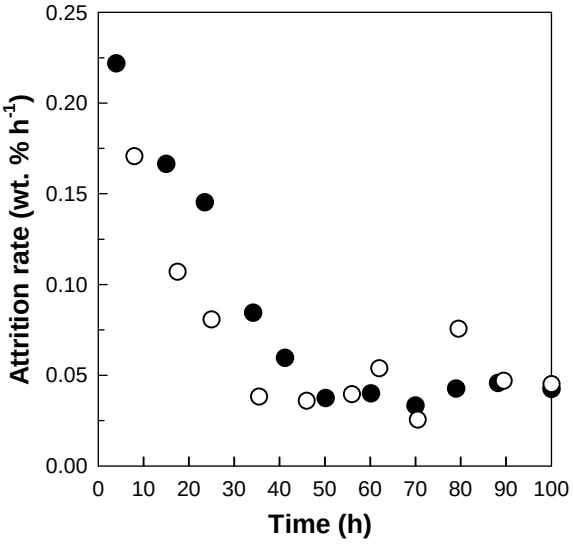
Attrition rate (wt. % h-1)
0.25
0.20
0.15
0.10
0.05
0.00
0
10
20
30
40
50
60
70
80
90
100
Time (h)

Figure 4

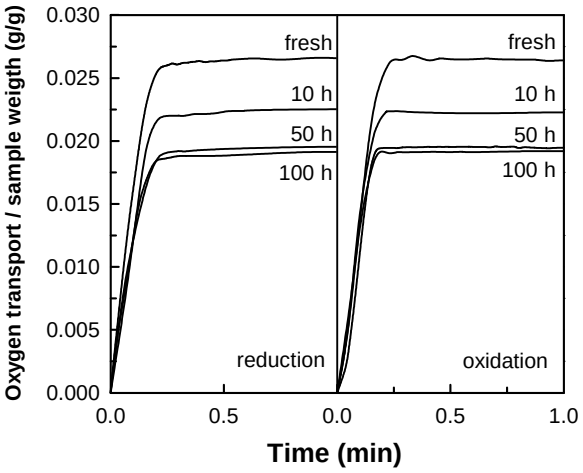
Oxygen transport / sample weigth (g/g)
0.030
0.025
0.020
0.015
0.010
0.005
0.000
fresh
10 h
50 h
100 h
reduction
oxidation
0.0
0.5
0.0
0.5
1.0
Time (min)

Figure 5

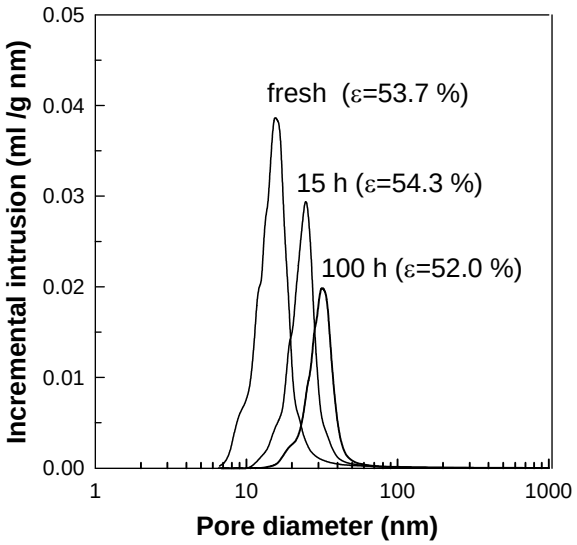
0.05
0.04
0.03
0.02
0.01
0.00
Incremental intrusion (ml /g nm)
fresh (ε=53.7 %)
15 h (ε=54.3 %)
100 h (ε=52.0 %)
1
10
100
1000
Pore diameter (nm)

Figure 6

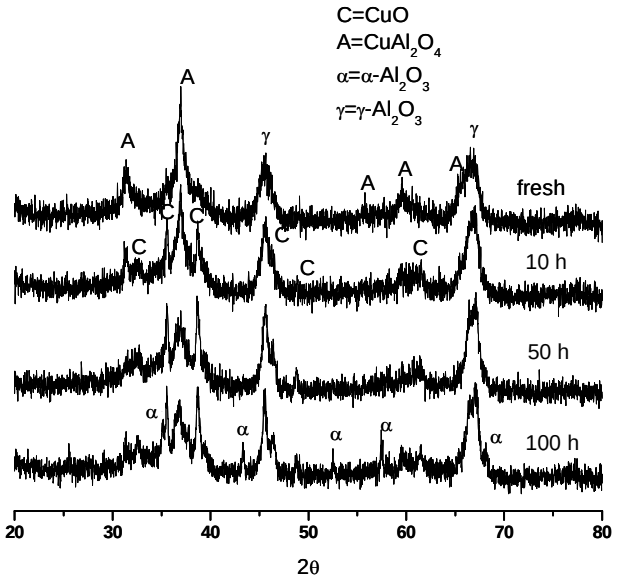
C=CuO
A=CuAl2O4
α=α-Al2O3
γ=γ-Al2O3
fresh
10 h
50 h
100 h
20
30
40
50
60
70
80
2θ

Figure 7

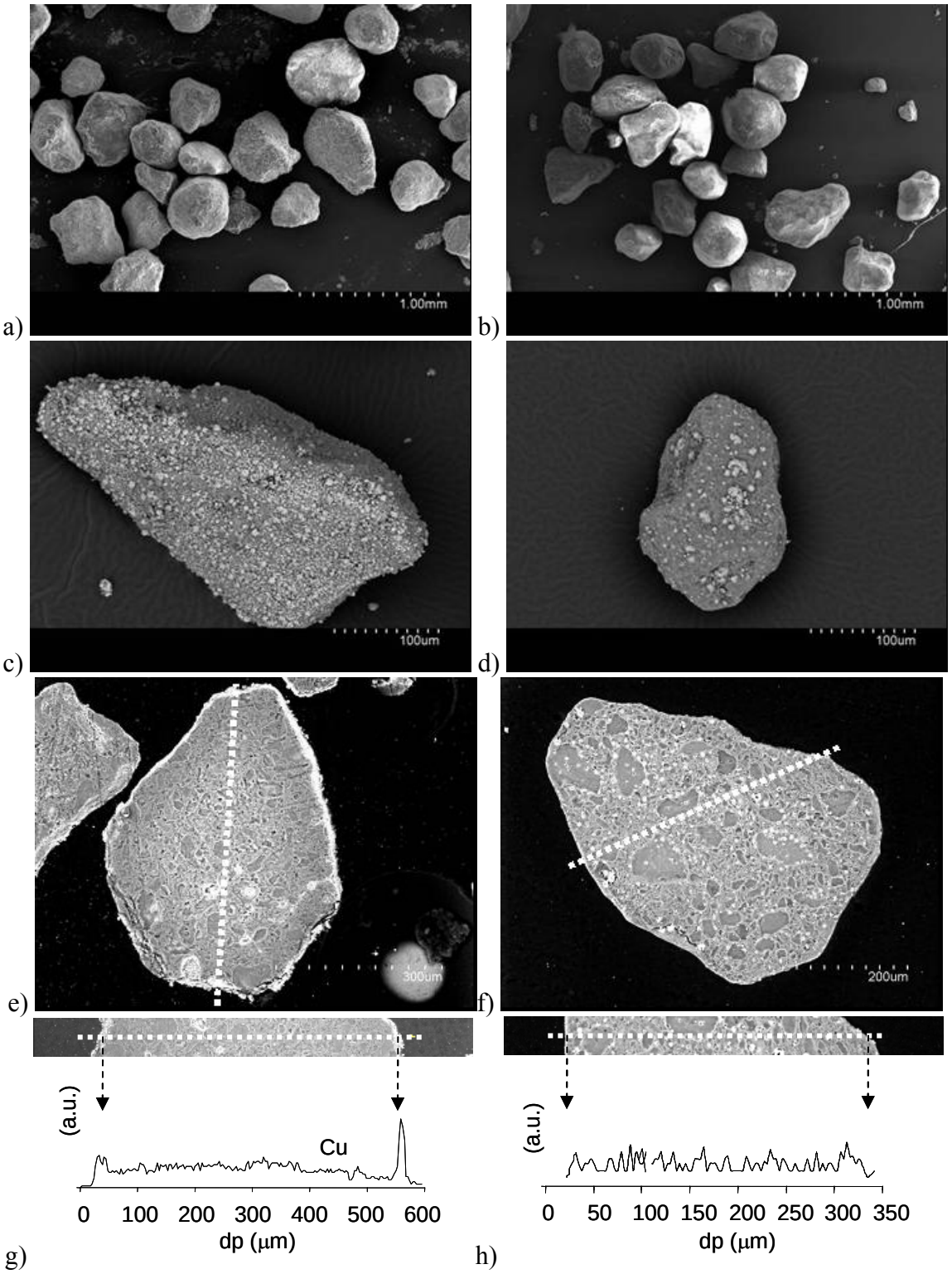
a)
1.00mm
b)
1.00mm
c)
100um
d)
100um
e)
300um
f)
200um
(a.u.)
Cu
0 100 200 300 400 500 600
dp (μm)
g)
(a.u.)
0 50 100 150 200 250 300 350
dp (μm)
h)